metal and O atoms are observed in Fig. 2. The results of the two kinds of ASF refinements showed that the wavefunctions based on the O_h crystal field are sufficient to describe the $3d$ electron distributions in a real crystal to a first approximation.

The electron population of the a_g orbital is smaller than that of the $e_g(t_{2g})$ orbitals, contradicting the estimated energy levels. Since the energy gap between these two orbitals is small, the order of the levels may be reversed when a closer approximation is adopted in the calculation. Another possibility of obtaining the reversed electron populations exists in the processing of the diffraction data. For example, the thermal diffuse scattering and anharmonic thermal vibrations of the atoms were not taken into account in the present study.

Part of the cost was met by a Grant-in-Aid for Scientific Research, No. 56420019, from The Ministry of Education, Science and Culture, to which the authors' thanks are due.

References

BECKER, P. J. & COPPENS, P. (1974*a*). *Acta Cryst.* **A30**, 129–147.
BECKER, P. J. & COPPENS, P. (1974*b*). *Acta Cryst.* **A30**, 148–153.
BECKER, P. J. & COPPENS, P. (1975). *Acta Cryst.* **A31**, 417–425.
BOND, W. L. (1951). *Rev. Sci. Instrum.* **22**, 344.
International Tables for X-ray Crystallography (1967). Vol. II, 2nd ed. Birmingham: Kynoch Press.
International Tables for X-ray Crystallography (1974). Vol. IV. Birmingham: Kynoch Press.
IWATA, M. (1977). *Acta Cryst.* **B33**, 59–69.
KIDOH, K., TANAKA, K., MARUMO, F. & TAKEI, H. (1983). To be published.
KOGURE, H. & TAKEUCHI, Y. (1983). Private communication.
LEWIS, J., SCHWARZENBACH, D. & FLACK, H. D. (1982). *Acta Cryst.* **A38**, 733–739.
MARUMO, F., ISOBE, M. & AKIMOTO, S. (1977). *Acta Cryst.* **B33**, 713–716.
TAKEI, H., HOSOYA, S. & KOJIMA, H. (1982). *J. Jpn. Assoc. Mineral Pet. Econ. Geol.* Special Issue 3, pp. 73–82.
TOKONAMI, M. (1965). *Acta Cryst.* **19**, 486.
VINCENT, M. G., YVON, K. & ASHKENAZI, J. (1980). *Acta Cryst.* **A36**, 808–813.
VINCENT, M. G., YVON, K., GRÜTTNER, A. & ASHKENAZI, J. (1980). *Acta Cryst.* **A36**, 803–808.
WEISS, R. J. & FREEMAN, A. J. (1959). *J. Phys. Chem. Solids*, **10**, 147–161.

Acta Cryst. (1984). B**40**, 96–102

Anharmonic Thermal Vibrations of Atoms in $MgAl_2O_4$ Spinel at Temperatures up to 1933 K

BY TAKAMITSU YAMANAKA, YOSHIO TAKÉUCHI AND MASAYASU TOKONAMI

Mineralogical Institute, Faculty of Science, University of Tokyo, Hongo, Tokyo, Japan

(*Received* 25 *August* 1983; *accepted* 8 *November* 1983)

Abstract

Anharmonic thermal vibrations of atoms in $MgAl_2O_4$ spinel ($Fd3m$, $Z=4$) have been studied using sets of accurate X-ray diffraction intensities of Bragg reflections at temperatures up to 1933 K. The study was initiated by refining the temperature factor $T(\mathbf{Q})$ of each atom in the form of the second-rank tensor β_{ij}, the ellipsoidal model of harmonic vibration being assumed. Difference Fourier maps based on the structure factors obtained from the refinements at 293 K ($R=0{\cdot}0197$), 1503 K ($R=0{\cdot}0413$), 1663 K ($R=0{\cdot}0432$) and 1933 K ($R=0{\cdot}0431$) revealed residual electron densities around the atoms at the tetrahedral site A (point symmetry $\bar{4}3m$) and octahedral site B ($\bar{3}m$) and also around the O atoms ($3m$), the models of occurrence suggesting anharmonic atomic thermal vibration. The observed intensities I_{obs} ($=I_{Bragg}+I_{TDS}$) were corrected for thermal diffuse scattering to extract the real intensities of the Bragg reflections. The correction was based on the one-photon and first-order acoustic vibration model. For the anharmonic refinement, a cumulant expansion of $T(\mathbf{Q})$ in the form $T(\mathbf{Q})=\exp[\sum_n (i^n/n!)\psi_{pqrs}\ldots q_p q_q q_r q_s\ldots]$ [Johnson (1969). *Acta Cryst.* **A25**, 187–194] was adopted. The coefficients of the anharmonic tensors of both tetrahedrally and octahedrally coordinated atoms were evaluated simultaneously at each temperature: 293 K ($R=0{\cdot}014$), 1503 K ($R=0{\cdot}027$), 1663 K ($R=0{\cdot}032$) and 1933 K ($R=0{\cdot}025$). In the difference Fourier maps after the anharmonic refinements, the above-mentioned residual electron densities disappeared. As the O positional parameters ($x\,x\,x$) have been found to be unaffected by the TDS correction, the A–O and B–O interatomic distances remain unchanged. These distances are, however, changed after the refinement for the anharmonic thermal vibrations of the atoms.

Introduction

According to the Debye–Waller theory assuming harmonic thermal motion of atoms, the temperature factor W_k is given by

$$W_k=\frac{8\pi^2\sin^2\theta}{\lambda^2}\langle u_k^2\rangle=B_k\sin^2\theta/\lambda^2, \qquad (1)$$

0108-7681/84/020096-07$01.50

where B_k is the isotropic temperature factor and $\langle u_k^2 \rangle$ the mean-square displacement of atom k (James, 1962). In the region of temperature T in which atomic thermal vibration can be expressed as an approximation of the harmonic oscillation, $\langle u^2 \rangle$ varies in proportion to T. The above approximation would no longer be satisfactory for the interpretation of diffraction intensities for thermal vibrations. We must therefore take into account anharmonic thermal vibrations of individual atoms in the unit cell when we deal with temperature factors. The analysis of the anharmonic thermal vibration of an atom in a crystal is not only an inevitable subject in the field of high-temperature crystal chemistry but also of basic importance to account for such thermal properties of the crystal as thermal expansion and thermal conductivity. Several theoretical approaches to the analysis of the anharmonic vibration have been tried to overcome the difficulty of the lattice-dynamic introduction of the anharmonicity into the probability density function (p.d.f.). The p.d.f. is defined by the time- and lattice-average densities of atoms in three-dimensional space. Anharmonic thermal vibration brings about a deviation of the p.d.f. from a Gaussian distribution. In order to evaluate the deviation, Johnson (1969, 1970) proposed a multimodal distribution using a cumulant expansion (Edgeworth expansion). Willis (1969) and Mair & Barnea (1975) introduced the anharmonic potential function for cubic symmetry to the p.d.f. by applying the Taylor expansion. Matsubara (1975) interpreted the anharmonicity by another type of potential function. Zucker & Schulz (1982) and Kuhs (1983) recommended the Gram–Charlier expansion with respect to a statistical approach for the treatment of anharmonicity.

As well as the correction for the anharmonic thermal motion, the effect of thermal diffuse scattering (TDS) on the diffraction intensities should be taken into account especially for the intensity measurements at high temperatures, because the effect becomes more conspicuous due to increasing atomic vibrations. Observed integrated intensities, I_{obs}, consist both of intensities I_{Bragg} of the Bragg reflection and I_{TDS} caused by thermal diffuse scattering in the background. The following equation then results

$$I_{obs} = I_{Bragg} + I_{TDS} = I_{Bragg}(1 + \alpha_1), \qquad (2)$$

where α_1 is a correction factor for TDS. The theory of TDS correction has been advanced by Skelton & Katz (1969), Rouse & Cooper (1969), Lucas (1969), Walker & Chipman (1970), Harada & Sakata (1974) and Merisalo & Kurittu (1978).

In a paper published elsewhere, we reported a series of structural studies of $MgAl_2O_4$ spinel and Mg_2SiO_4 olivine at high temperatures (Takéuchi, Yamanaka, Haga & Hirano, 1983). We now present the result of the analysis of the anharmonic thermal vibration of the atoms in the spinel structure by means of X-ray diffraction intensities collected at temperatures up to 1933 K. $MgAl_2O_4$ spinel has a normal spinel arrangement (Bacon, 1952): the Mg atom is at the tetrahedral site (A site) with point symmetry $\bar{4}3m$, Al is at the octahedral site (B site) with symmetry $\bar{3}m$, and the O atom is at the position ($x\,x\,x$) with point symmetry $3m$. However, an order–disorder transition at around 973 K was reported by Suzuki & Kumazawa (1980) and Yamanaka & Takéuchi (1983). Recently, Grimes, Thompson & Kay (1983) reported that the space group of $MgAl_2O_4$ was $F\bar{4}3m$ rather than $Fd3m$. We adopted the latter space group which has hitherto been assigned to the spinel structure. According to Baumgartner, Preisinger, Heger & Guth (1981) the space group of spinel changes to $Fd3m$ above 1023 K.

On the basis of the intensities resulting after correction for TDS, the analysis of the anharmonic thermal vibration of the atoms at both tetrahedral and octahedral sites has been investigated simultaneously as a function of temperature. Not only the results of the corrected refinements but also their comparison with the regular uncorrected refinements are presented below.

Measurements of X-ray diffraction intensity

A spherically shaped crystal having a diameter of 0·2 mm was prepared from a flux-grown stoichiometric spinel crystal of $MgAl_2O_4$. X-ray diffraction intensities were collected on a Syntex $P2_1$ four-circle diffractometer, using Mo $K\alpha$ radiation monochromated by pyrolytic graphite. The ω–2θ scanning mode was employed at $1^\circ\,min^{-1}$ in 2θ. Diffraction intensity measurements at temperatures higher than 1273 K were carried out using a gas-flame heating system (Yamanaka, Takéuchi & Sadanaga, 1981). At each temperature studied a total of about 100 intensities were measured in the range $0{\cdot}12 < \sin\theta/\lambda < 1{\cdot}41$ Å^{-1} and were corrected for Lorentz and polarization effects and for absorption.*

Difference Fourier synthesis as a function of temperature

The structure refinements including anisotropic temperature parameters (β_{ij}) and an isotropic-extinction parameter (ΔG) were conducted using the full-matrix least-squares program *LINUS* (Coppens & Hamilton, 1970). Mean atomic scattering factors of fully ionized Mg^{2+} and Al^{3+} and their dispersion factors were taken from *International Tables for X-ray Crystallography* (1962) and that of O^{2-} from Tokonami (1965). Results

* Lists of structure factors have been deposited with the British Library Lending Division as Supplementary Publication No. SUP 38970 (5 pp.). Copies may be obtained through The Executive Secretary, International Union of Crystallography, 5 Abbey Square, Chester CH1 2HU, England.

Table 1. *Refinement conditions and refined structure parameters with and without the TDS correction*

A figure in parentheses indicates the standard deviation in the least-squares calculation. Isotropic temperature parameters are calculated from the anisotropic temperature parameters. The extinction parameter is not refined in the refinement with TDS correction.

Temperature (K)	293		1503		1663		1933	
a (Å)	8·0806 (5)		8·1740 (13)		8·1860 (10)		8·2065 (12)	
Reflections used	145		91		130		89	
2θ (°)	100		80		100		80	
		TDS		TDS		TDS		TDS
R (%)	1·97	1·85	4·13	2·70	4·32	3·57	4·31	3·16
R_w (%)	1·91	1·46	4·67	2·67	4·11	2·89	4·14	2·66
O ($x\,x\,x$)	0·3873 (1)	0·3873 (1)	0·3862 (2)	0·3863 (2)	0·3860 (1)	0·3859 (1)	0·3857 (2)	0·3855 (1)
Extinction parameter $\times 10^6$	0·233 (3)	—	0·311 (28)	—	0·224 (11)	—	0·488 (31)	—
$\beta_{11}(A)\times 10^5$	230 (4)	237 (3)	618 (14)	647 (6)	680 (7)	702 (6)	786 (10)	798 (6)
$\beta_{11}(B)\times 10^5$	248 (3)	252 (2)	628 (10)	651 (4)	693 (5)	712 (4)	810 (6)	833 (4)
$\beta_{12}(B)\times 10^5$	−7 (7)	−7 (7)	−51 (18)	−50 (11)	−61 (14)	−58 (10)	−72 (18)	−67 (13)
$\beta_{11}(O)\times 10^5$	333 (4)	338 (3)	779 (14)	798 (7)	863 (9)	879 (7)	974 (12)	995 (7)
$\beta_{12}(O)\times 10^5$	−5 (4)	−13 (3)	−32 (12)	−40 (7)	−25 (9)	−40 (7)	−27 (12)	−39 (9)
$B(A)$	0·56	0·60	1·65	1·73	1·82	1·88	2·11	2·14
$B(B)$	0·61	0·66	1·68	1·74	1·86	1·91	2·18	2·13
B(O)	0·85	0·88	2·08	2·14	2·31	2·34	2·62	2·67

of the refinements are presented in Table 1. Difference Fourier syntheses based on F_c and F_o obtained at 293, 1503, 1663 and 1933 K, as shown in Fig. 1, exhibit the following features.

(1) Residual electron densities were observed around the A ($\bar{4}3m$), B ($\bar{3}m$) and O ($3m$) sites of the spinel structure at temperatures higher than 1473 K.

(2) These positive peaks appear around the A sites and O atoms on the opposite side of each tetrahedral bond, showing a tetrapod-shaped electron density around each atom. With respect to the B sites, the positive peaks appear in a region free from the bonds to the neighbors, indicating eight lobes along [111] of the octahedral coordination. Negative peaks are located on the bonds around all atoms.

(3) Heights of the positive and negative peaks are intensified progressively with increasing temperature and the peak positions are displaced from the centers of the atoms, as seen from Table 2.

(4) The above features are noticeable particularly at the A site which has noncentrosymmetric site symmetry $\bar{4}3m$.

The above features observed in the difference Fourier maps may be interpreted in two ways: one is

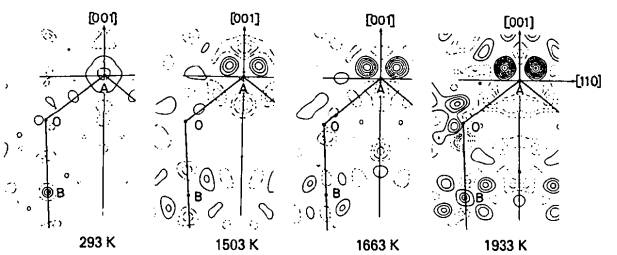

Fig. 1. Difference Fourier maps of $MgAl_2O_4$ at different temperatures, each showing a section passing through the A site and parallel to (110). These maps are based on the refinements including the harmonic temperature parameters. Contours are drawn at intervals of 0·2 e Å^{-3}, starting from the 0·2 e Å^{-3} contour. Positive and negative contours are presented by solid and broken lines, respectivey; the zero contour is omitted.

Table 2. *Heights and distances on the difference electron density map*

	A site ($\bar{4}3m$)		B site ($\bar{3}m$)	
	Δd (Å)*	eÅ^{-3}	Δd (Å)*	eÅ^{-3}
1503 K	0·448	0·3	0·607	0·2
1663 K	0·472	0·5	0·540	0·2
1933 K	0·513	0·7	0·638	0·3

* The distance is from the center of the residual peak to the atomic position.

static disorder (lattice average) and the other dynamical disorder (time average) of the atoms in the crystal structure. The mode of temperature dependence of the residual electron densities seems to suggest that the latter is more likely and they will be ascribed to the anharmonic contribution to the thermal vibrations. It is unnecessary to consider localization of bonding electrons, lone-pair electrons or aspherical distributions of d electrons in the present case of $MgAl_2O_4$. Consequently, further refinements introduce a statistical approach to the analysis of anharmonic thermal motion, such as that developed by Johnson (1969, 1970).

Correction for thermal diffuse scattering

Since diffraction intensities were measured at temperatures up to 1933 K, the correction for thermal diffuse scattering (TDS) affecting the intensities should be made before the refinements considering the anharmonicity in temperature factors.

Since the intensities of the first-order scattering by acoustic lattice vibration have a maximum peak at the reciprocal-lattice point, it is convenient for the calculation of the TDS correction to express the elastic wavevector by the reflection indices hkl and the reciprocal axes a^*, b^*, c^*, providing that the Cartesian axes x, y, z of the elastic wave are chosen in exact conformity with the crystal axes a, b, c. For this purpose we can simply adopt the UB matrix (Busing & Levy, 1967) used for intensity measurement

Table 3. *Elastic constants of* $MgAl_2O_4$ *at* 298 K *and their temperature derivatives (after Chang & Barch, 1973)*

$c_{11} = 2{\cdot}8248\,(56) \times 10^{10}$ Pa	$(\partial c_{11}/\partial T)_P = -0{\cdot}262 \times 10^{10}$ Pa K^{-1}
$c_{12} = 1{\cdot}5491\,(48)$	$(\partial c_{12}/\partial T)_P = -0{\cdot}0997$
$c_{44} = 1{\cdot}5468\,(19)$	$(\partial c_{44}/\partial T)_P = -0{\cdot}0878$

with the four-circle diffractometer. Once the coordinate system is so chosen, the elastic tensors c_{ij} ($i, j = 1, 6$) numerically coincide with the elastic constants. Three independent elastic constants c_{11}, c_{12} and c_{44} for $MgAl_2O_4$ and their temperature derivatives were determined by Chang & Barch (1973) using the ultrasonic pulse superposition method (Table 3). The elastic constants at high temperatures are calculated from the linear extrapolation of the temperature derivatives.

The computer program *SXTDS*1 (Kurittu & Merisalo, 1977) was used for the evaluation of the correction factor α_1. This evaluation involved not only the elastic constants and the direction cosines of the reflections derived from the *UB* matrix, but also such experimental parameters as the scanning mode ω–2θ, the scan width, and the receiving-slit width. Structure factors F_{Bragg} can be evaluated from the intensities derived from the Bragg reflections alone, which are extracted from the observed integrated intensities (I_{obs}) after making the TDS correction. With respect to the diffraction intensities measured at 293, 1503, 1663 and 1933 K, the difference between F_{Bragg} and F_{obs}, that is $\Delta F = F_{\text{obs}} - F_{\text{Bragg}}$, is an error present in the structure factor F_{obs} which is obtained from I_{obs} ($= I_{\text{Bragg}} + I_{\text{TDS}}$). In Fig. 2 we give a plot of the values of $\Delta F/F_{\text{Bragg}} \times 100(\%)$ [$\Delta F/F_{\text{Bragg}} = \sqrt{(1+\alpha_1)} - 1$] *versus* $\Sigma = h_i^2 + k_i^2 + l_i^2$ shown as the abscissa. As clearly seen from Fig. 2, $\Delta F/F_{\text{Bragg}}$ increases with increasing temperature because of the linear decrease of c_{ij}, which in turn leads to the elevation of the factor α_1. Since α_1 has a positive correlation with the square summation of h_i, k_i and l_i, reflections with higher-order indices give larger values of $\Delta F/F_{\text{Bragg}}$. All reflections having the same Σ value do not necessarily exhibit the same value of $\Delta F/F_{\text{Bragg}}$. This may be ascribed to the fact that the elastic tensors c_{ij} even in the cubic crystal are not isotropic. Therefore, reflections, even though having the same value of $\sin\theta/\lambda$, have different correction factors α_1.

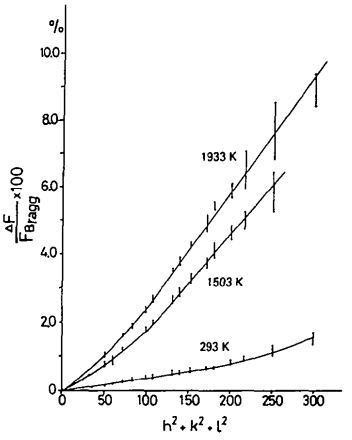

Fig. 2. Error in the structure factor caused by the TDS effect. $F_{\text{obs}} - F_{\text{Bragg}}$ is represented by ΔF. $\Delta F/F_{\text{Bragg}}$ of the reflections having the same $h^2+k^2+l^2$ are joined by the vertical line.

Since the crystal of $MgAl_2O_4$ is a fairly hard material having a large value of c_{ij} at room temperature, the diffraction intensities of even higher-angle reflections are little affected by TDS, indicating $\Delta F/F_{\text{Bragg}} < 0{\cdot}02$. At high temperatures, however, the reflections are noticeably affected by TDS. For instance, $\Delta F/F_{\text{Bragg}}$ of the higher-order indices is as much as 0·1, especially at such a high temperature as 1933 K.

The TDS correction was carried out in accordance with the assumption that the elastic constants c_{ij} at high temperatures can be calculated using the appropriate temperature derivatives. In addition, the correction was based on the theory of TDS for a perfect crystal, in which elastic waves propagate homogeneously. Accordingly, it is noted that the observed diffraction intensities tend to be corrected excessively.

The results of the refinements after the TDS correction are given in Table 1 together with those before the TDS correction. Reliability factors (R factors) for the least-squares refinements decreased after the TDS corrections for each temperature, thereby indicating more precise structure parameters. Only the variable positional parameters ($x\,x\,x$) for the O atoms did not change after the correction. However, the anisotropic temperature parameters, namely β_{ij} ($i, j = 1, 3$), all increased. As expected, therefore, the isotropic temperature parameters of those atoms also increased.

The TDS correction factor α_1 and the Debye–Waller factor $W(\mathbf{Q})$ are both expressed by the similar formalism regarding h_i, k_i and l_i, regardless of atomic positional parameters. Therefore, only a term of $W(\mathbf{Q})$ is corrected by the TDS correction. The results of the refinements, shown in Table 1, after the TDS correction are not contradictory to the above explanation.

In the difference Fourier maps obtained from F_{calc} and previously corrected F_{obs}, both positive and negative peaks in the background disappear and the peaks presumably caused by the anharmonic thermal vibrations of the atoms also fall in height. For instance, the difference Fourier map resulting from the TDS correction to the set of the diffraction intensities at 1933 K is presented in Fig. 3.

As indicated in Table 1 and Fig. 2, the structure refinement of the hard ionic crystal at room temperature requires little TDS correction, but TDS markedly affects the diffraction intensity measured at high temperatures.

Anharmonic thermal vibration

The present study was initiated by refining the temperature factor in the 'harmonic approximation', in which all terms higher than second order were ignored. We now consider the higher-order terms to study the influence of anharmonicity on the diffraction intensities of $MgAl_2O_4$. Among various approaches to the anharmonic refinement, we adopted a multimodal distribution in the p.d.f. developed by Johnson (1969, 1970). The present structure refinements are carried out using the following structure-factor formalism:

$$F = \sum_j f_j \exp(2\pi i \sum H_p x_p^j) T(\mathbf{H}). \quad (3)$$

The temperature factor $T(\mathbf{H})$ is derived from the cumulant expansion

$$T(\mathbf{H}) = \exp\left(\frac{i^2}{2!}\sum_p\sum_q \mathbf{B} H_p H_q + \frac{i^3}{3!}\sum_p\sum_q\sum_r \mathbf{C} H_p H_q H_r + \frac{i^4}{4!}\sum_p\sum_q\sum_r\sum_s \mathbf{D} H_p H_q H_r H_s + \cdots\right) \quad (4)$$

where **B**, **C**, **D**, ... are respectively the second-, third-, fourth-order ... coefficients of cumulant expansion and indicate the anharmonic thermal tensors. The coefficients higher than fifth order were neglected in variable parameters of the expansion, because these coefficients were regarded as practically meaningless and hardly converged in the least-squares calculation due to their correlations. **B**, **C**, **D**, ... are the coefficient tensors, namely, six tensors of β_{ij} belong to **B**; ten tensors of γ_{ijk} to **C** and fifteen tensors of δ_{ijkl} to **D**. These tensors are constrained according to the point symmetry of the atomic sites. The site-symmetry constraints on thermal-motion tensor coefficients are set forth in *International Tables for X-ray Crystallography* (1962). With respect to the space group $Fd3m$ of $MgAl_2O_4$ having site symmetry $\bar{4}3m$ for the *A* sites, $\bar{3}m$ for the *B* sites, and $3m$ for the O sites, the constraints of the tensors are presented in Table 4, in which independent variable coefficients and their covariants are also listed.

Using the diffraction intensities corrected for TDS, the structure refinement including the above anharmonic tensors for the temperature factors of the atoms was conducted with the computer program originally written by Finger & Prince (1975), which applies the cumulant expansion to the temperature factor. The results of the refinements (Table 5) reveal several

Table 4. *Site-symmetry restrictions on thermal-motion tensor coefficients*

	Order	
A site ($\bar{4}3m$)	2nd	$\beta_{11} = \beta_{22} = \beta_{33}$
	3rd	γ_{123}
	4th	$\delta_{1111} = \delta_{2222} = \delta_{3333}$ $\delta_{1122} = \delta_{1133} = \delta_{2233}$
B site ($\bar{3}m$)	2nd	$\beta_{11} = \beta_{22} = \beta_{33}$ $\beta_{12} = \beta_{13} = \beta_{23}$
	4th	$\delta_{1111} = \delta_{2222} = \delta_{3333}$ $\delta_{1112} = \delta_{1222} = \delta_{1113} = \delta_{1333} = \delta_{2223} = \delta_{2333}$ $\delta_{1122} = \delta_{1133} = \delta_{2233}$ $\delta_{1123} = \delta_{1223} = \delta_{1233}$
O ($3m$)	2nd	$\beta_{11} = \beta_{22} = \beta_{33}$ $\beta_{12} = \beta_{13} = \beta_{23}$
	3rd	$\gamma_{111} = \gamma_{222} = \gamma_{333}$ $\gamma_{112} = \gamma_{122} = \gamma_{113} = \gamma_{133} = \gamma_{223} = \gamma_{233}$ γ_{123}
	4th	$\delta_{1111} = \delta_{2222} = \delta_{3333}$ $\delta_{1112} = \delta_{1222} = \delta_{1113} = \delta_{1333} = \delta_{2223} = \delta_{2333}$ $\delta_{1122} = \delta_{1133} = \delta_{2233}$ $\delta_{1123} = \delta_{1223} = \delta_{1233}$

Table 5. *Structure parameters obtained from the anharmonic refinement*

Temperature (K)	293	1503	1663	1933
R (%)	1·41	2·73	3·17	2·50
R_w (%)	1·32	2·43	2·88	2·39
O ($x\,x\,x$)	0·3871 (1)	0·3860 (1)	0·3857 (1)	0·3850 (1)
$\beta_{11}(A)\times10^5$	234 (9)	607 (26)	694 (18)	790 (21)
$\gamma_{123}(A)\times10^6$	−2 (4)	22 (9)	31 (8)	49 (14)
$\delta_{1111}(A)\times10^7$	0 (5)	−43 (18)	−20 (15)	−41 (18)
$\delta_{1122}(A)\times10^7$	−1 (2)	10 (7)	10 (5)	18 (7)
$\beta_{11}(B)\times10^5$	284 (7)	619 (21)	725 (14)	818 (17)
$\beta_{12}(B)\times10^5$	−10 (5)	−66 (10)	−66 (8)	−82 (9)
$\delta_{1111}(B)\times10^7$	−20 (3)	−30 (13)	−14 (10)	−14 (11)
$\delta_{1112}(B)\times10^7$	−2 (2)	−5 (4)	−3 (3)	−3 (4)
$\delta_{1122}(B)\times10^7$	7 (2)	13 (5)	14 (3)	13 (4)
$\delta_{1123}(B)\times10^7$	1 (1)	−5 (3)	1 (2)	−6 (5)
$\beta_{11}(O)\times10^5$	390 (5)	767 (30)	926 (20)	990 (21)
$\beta_{12}(O)\times10^5$	−7	43 (18)	−37 (16)	−41 (17)
$\gamma_{111}(O)\times10^6$	12 (6)	48 (13)	48 (8)	125 (17)
$\gamma_{112}(O)\times10^6$	3 (3)	−6 (10)	−22 (16)	−19 (8)
$\gamma_{123}(O)\times10^6$	9 (5)	25 (12)	14 (6)	4 (20)
$\delta_{1111}(O)\times10^7$	32 (5)	−33 (22)	−16 (17)	−5 (19)
$\delta_{1112}(O)\times10^7$	1 (2)	−5 (7)	2 (6)	−5 (7)
$\delta_{1122}(O)\times10^7$	9 (2)	14 (8)	15 (6)	10 (9)
$\delta_{1123}(O)\times10^7$	−1 (2)	−4 (5)	−10 (5)	−7 (9)

Figures in parentheses indicate the standard deviations in the last cycle of least-squares refinement. Refinement conditions are as in Table 1.

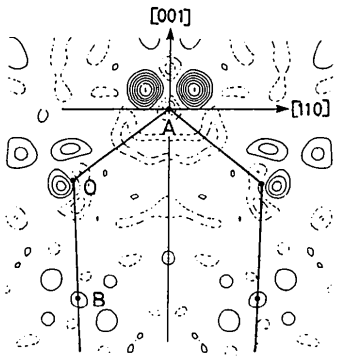

Fig. 3. Difference Fourier map after the TDS correction at 1933 K. The Fourier section and contour interval are as in Fig. 1.

differences in the structure parameters from those of the regular refinements based on the ellipsoidal harmonic thermal vibrations of the atoms (Table 1).

In comparison with the case of harmonic refinements, the values of R are markedly reduced: from 1·97 to 1·41% at 293 K, from 4·13 to 2·73% at 1503 K, from 4·32 to 3·17% at 1663 K and from 4·31 to 2·50% at 1933 K. The results presumably indicate that the analysis of the anharmonicity assures a better structure refinement.

When anharmonic terms for each atom are introduced, the second-order tensors of the cumulants, corresponding to the anisotropic temperature factors β_{ij}, show more intense anisotropy especially in the refinements at high temperatures. The anharmonic refinement renders the anisotropy of the temperature factors more noticeable. Atoms at the A sites show a large value of γ_{123} indicating that the thermal motion may well be represented by the shape of a tetrapod, while those at B show a relatively large δ_{1122}, thermal motion being represented by a set of eight lobes along the lines parallel to the cubic body diagonals. The O atoms show a conspicuous anisotropic anharmonicity at 1933 K. The higher the temperature, the more marked is the anharmonicity of the atomic thermal vibration.

In the difference Fourier maps after the anharmonic refinements, residual electron densities around the atoms almost entirely disappeared, as shown for example at 1933 K (Fig. 4). The above fact suggests that this treatment of the anharmonic thermal vibrations of the atoms results in a most reliable refinement. The atomic position of O ($x\,x\,x$) obtained from the anharmonic refinement is different from that determined by the harmonic refinement. This leads to the fact that the interatomic distances are different before and after the anharmonic refinement, because the distances vary with the x parameter and the lattice constant. Bond distances A–O and B–O, and shared $(O–O)_{sh}$ and unshared $(O–O)_{unsh}$ edge distances of the octahedral site, and $(O–O)_{tet}$ tetrahedral-edge distances are presented in Table 6, in comparison with those distances from the harmonic refinements. The A–O and B–O distances (Fig. 5) are contracted and slightly lengthened, respectively, after the anharmonic refinement. Therefore, the thermal-expansion coefficients of each bond must take into account the effect of the anharmonic thermal vibration of the atom. The thermal expansion of the lattice parameter results from the anharmonic vibration, especially of O atoms that form the cubic close packing in the spinel structure.

Table 6. *Selected interatomic distances* (Å) *resulting from the harmonic and anharmonic refinements*

Temperature (K)	293	1503	1663	1933
$(A–O)_{anh}$	1·9188 (7)	1·9260 (12)	1·9242 (11)	1·9183 (13)
$(A–O)_{h}$	1·9221 (8)	1·0283 (15)	1·9283 (14)	1·9288 (14)
Δd	−0·0033	−0·0017	−0·0041	−0·0105
$(B–O)_{anh}$	1·9273 (8)	1·9562 (12)	1·9627 (12)	1·9733 (13)
$(B–O)_{h}$	1·9257 (8)	1·9562 (15)	1·9606 (14)	1·9677 (14)
Δd	0·0016	0·0012	0·0021	0·0056
$(O–O)_{tet,anh}$	3·1335 (11)	3·1452 (20)	3·1422 (18)	3·1324 (21)
$(O–O)_{tet,h}$	3·1388 (13)	3·1488 (21)	3·1489 (20)	3·1497 (20)
Δd	−0·0053	−0·0036	−0·0067	−0·0173
$(O–O)_{sh,anh}$	2·5804 (10)	2·6347 (18)	2·6462 (17)	2·6702 (20)
$(O–O)_{sh,h}$	2·5751 (11)	2·6257 (20)	2·6395 (20)	2·6531 (20)
Δd	0·0053	0·0088	0·0067	0·0171
$(O–O)_{unsh,anh}$	2·8636 (11)	2·8956 (21)	2·8995 (18)	2·9060 (21)
$(O–O)_{unsh,h}$	2·8639 (11)	2·8959 (21)	2·8998 (20)	2·9066 (20)
Δd	−0·0003	−0·0003	−0·0003	−0·0006

$(O–O)_{sh}$, $(O–O)_{unsh}$ and $(O–O)_{tet}$ indicate the shared and unshared edge of the octahedron around the B site and the edge of the tetrahedron around the A site. h: harmonic; anh: anharmonic.

In our earlier paper (Yamanaka & Takéuchi, 1983) we proposed a second-order transition in $MgAl_2O_4$ taking place at 873–973 K due to the cation exchange of ^{IV}Mg and ^{VI}Al at the A and B sites. Although the inversion parameter i in $(Mg_{1-i}Al_i)$ $[Al_{2-i}Mg_i]O_4$ could not be determined directly from the refinement because of insignificant difference in X-ray scattering power between Mg^{2+} and Al^{3+}, the parameter could be estimated from the bond distances A–O and B–O

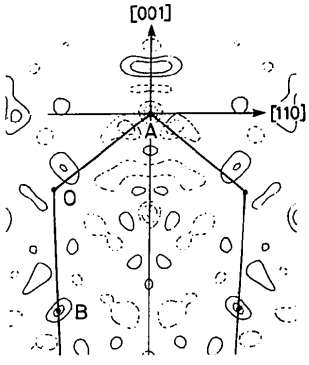

Fig. 4. Difference Fourier map after the TDS correction and anharmonic refinement at 1933 K. The Fourier section and contour interval are as in Fig. 1.

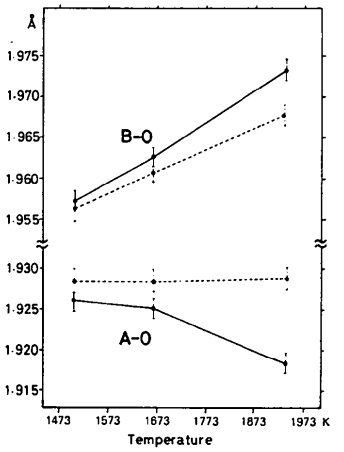

Fig. 5. Bond distances A–O and B–O obtained by the harmonic (broken line) and anharmonic refinements (solid line).

and their thermal-expansion coefficients. Since, as mentioned above, the bond distances after the anharmonic refinement are different from those obtained by the harmonic refinement, the inversion parameter of the cation ordering may be influenced.

More precise analysis of the anharmonic thermal vibration of atoms in addition to a study of the cation distribution will be carried out in the near future at high temperatures with neutron diffraction, in which large differences in cross section of Mg and Al can be effective in the above studies.

The authors are indebted to Professor C. T. Prewitt, State University of New York at Stony Brook, for his critical reviewings to improve the manuscript and to Dr Kihara, University of Kanazawa, for providing the program *SXTDS*1. They also wish to thank Professor R. Sadanaga, MJA, for his kind encouragement and interest during the progress of this work.

References

BACON, G. E. (1952). *Acta Cryst.* **5**, 684–686.
BAUMGARTNER, O., PREISINGER, A., HEGER, G. & GUTH, H. (1981). *Acta Cryst.* A**37**, C187.
BUSING, W. R. & LEVY, H. A. (1967). *Acta Cryst.* **22**, 457–464.
CHANG, Z. P. & BARCH, G. P. (1973). *J. Geophys. Res.* **78**, 2418–2433.
COPPENS, P. & HAMILTON, W. C. (1970). *Acta Cryst.* A**26**, 71–83.
FINGER, L. W. & PRINCE, E. (1975). *Natl Bur. Stand. (US) Tech. Note* 854.
GRIMES, N. W., THOMPSON, P. & KAY, H. F. (1983). *Proc. R. Soc. London Ser. A*, **386**, 333–345.
HARADA, J. & SAKATA, M. (1974). *Acta Cryst.* A**30**, 77–82.
International Tables for X-ray Crystallography (1962). Vol. III. Birmingham: Kynoch Press.
JAMES, R. W. (1962). *The Optical Principles of the Diffraction of X-rays*. London: Bell.
JOHNSON, C. K. (1969). *Acta Cryst.* A**25**, 187–194.
JOHNSON, C. K. (1970). *Thermal Neutron Diffraction*, edited by B. T. M. WILLIS, pp. 132–160. Oxford Univ. Press.
KUHS, W. F. (1983). *Acta Cryst.* A**39**, 148–158.
KURITTU, J. & MERISALO, M. (1977). *Report Series in Physics.* 132. Univ. Helsinki.
LUCAS, B. W. (1969). *Acta Cryst.* A**25**, 627–631.
MAIR, S. L. & BARNEA, Z. (1975). *Acta Cryst.* A**31**, 201–207.
MATSUBARA, T. (1975). *Prog. Theor. Phys.* **53**, 1210–1211.
MERISALO, M. & KURITTU, J. (1978). *J. Appl. Cryst.* **11**, 179–182.
ROUSE, K. D. & COOPER, M. J. (1969). *Acta Cryst.* A**25**, 615–621.
SKELTON, E. F. & KATZ, L. (1969). *Acta Cryst.* A**25**, 319–329.
SUZUKI, I. & KUMAZAWA, M. (1980). *Phys. Chem. Miner.* **5**, 279–284.
TAKÉUCHI, Y., YAMANAKA, T., HAGA, N. & HIRANO, M. (1983). *Materials Science of the Earth Interior*, edited by I. SUNAGAWA. Tokyo/Amsterdam: Terra/Leidel. In the press.
TOKONAMI, M. (1965). *Acta Cryst.* **19**, 486.
WALKER, C. B. & CHIPMAN, D. R. (1970). *Acta Cryst.* A**26**, 447–455.
WILLIS, B. T. M. (1969). *Acta Cryst.* A**25**, 277–300.
YAMANAKA, T. & TAKÉUCHI, Y. (1983). *Z. Kristallogr.* In the press.
YAMANAKA, T., TAKÉUCHI, Y. & SADANAGA, R. (1981). *Z. Kristallogr.* **154**, 147–153.
ZUCKER, U. H. & SCHULZ, H. (1982). *Acta Cryst.* A**38**, 563–568.

Acta Cryst. (1984). B**40**, 102–105

Das Entwässerungsverhalten des Natriummetavanadatdihydrats und die Kristallstruktur des β-Natriummetavanadats

VON KATSUO KATO UND EIJI TAKAYAMA

*Mukizaishitsu Kenkyusho,** 1-1 *Namiki, Sakura-mura, Niihari-gun, Ibaraki-ken* 305, *Japan*

(*Eingegangen am* 19. *August* 1983; *angenommen am* 11. *November* 1983)

Abstract

β-$NaVO_3$, $M_r = 121{\cdot}984$, orthorhombic, *Pnma*, $a = 14{\cdot}147\,(2)$, $b = 3{\cdot}6496\,(6)$, $c = 5{\cdot}364\,(1)$ Å, $V = 276{\cdot}96\,(9)$ Å^3, $Z = 4$, $D_x = 2{\cdot}924$ Mg m^{-3}, λ(Cu $K\bar{\alpha}$) = 1·5418 Å for measuring lattice constants, λ(Mo $K\bar{\alpha}$) = 0·71073 Å for intensity collection, $F(000) = 232$, $R = 0{\cdot}094$, 185 unique reflections. The sample was an aggregate of oriented crystallites obtained through topotactic dehydration of synthetic $NaVO_3.2H_2O$. The infinite metavanadate chains inherited from the hydrate run parallel to [010] and are bound together by Na ions. Within a chain, each V atom is surrounded by five O atoms to form a distorted trigonal bipyramid. The structure is oriented to the monoclinic hydrate (H) structure in such a way that strictly $[010]_\beta \| [010]_H$ and approximately $[00\bar{1}]_\beta \| [100]_H$ and $[101]_\beta \| [001]_H$. The dehydration probably proceeds through an intermediate stage.

Einleitung

Von Natriummetavanadat sind zwei Modifikationen bekannt (Lukács & Strusievici, 1962). Die Hochtemperaturform α kristallisiert monoklin in einer diopsid-ähnlichen Struktur. Bei einer Strukturverfeinerung dieser Form nahmen Marumo, Isobe, Iwai & Kondo (1974) die Raumgruppe $C2/c$ an. Dagegen

* Staatliches Institut für Anorganische Materialforschung.

0108-7681/84/020102-04$01.50